Biosystems Engineering (2004) **87** (3), 375–386
doi:10.1016/j.biosystemseng.2003.12.001
SW—Soil and Water

Interface Pressures of a Tractor Drive Tyre on Structured and Loose Soils

Thomas R. Way[1]; Tadashi Kishimoto[2]

[1] USDA-ARS National Soil Dynamics Laboratory, Auburn, AL 36832-5806, USA; e-mail of corresponding author: tway@ars.usda.gov
[2] Department of Food Production Science, Obihiro University of Agriculture and Veterinary Medicine, Inada-cho, Hokkaido, 080-8555 Japan; e-mail: tksmt@obihiro.ac.jp

(Received 20 March 2003; accepted in revised form 1 December 2003; published online 3 February 2004)

An 18·4R38 radial-ply tractor drive tyre was operated at 10% travel reduction, at three correctly inflated combinations of dynamic load and inflation pressures on a structured clay soil and at another combination of load and inflation pressure on a loose sandy loam and a loose clay loam soil. Soil–tyre interface pressures on the face of one lug and on an undertread region between two lugs were measured, and were used in estimating the tyre footprint area for the operating tyre. On the structured clay soil, the interface pressures on the lug face were substantially greater than tyre inflation pressure and those on the undertread were considerably less than inflation pressure. On the loose sandy loam and the loose clay loam, some interface pressures on the lug face exceeded inflation pressure by only a small amount and others were a small amount less than inflation pressure, while undertread pressures were less than inflation pressure. Tyre footprint areas on the structured clay soil were nearly equal for the three correctly inflated load and inflation pressure combinations. The footprint area on the loose sandy loam was 10% greater, and that on the loose clay loam was 4% greater, than the average of the three footprint areas on the structured clay soil.
Published by Elsevier Ltd on behalf of Silsoe Research Institute

1. Introduction

As reduced tillage farming systems have become more widespread, there has been an increase in the proportion of tractor operations occurring on soils which have not been tilled for periods of several months or longer. These soils typically have more soil structure than tilled soils and this structure affects the soil compaction characteristics and the tractive performance of tractors and other vehicles on the soil. Pressures applied to the soil surface by tractor drive tyres are an important factor affecting soil compaction and tractive performance.

Soil–tyre interface pressures of a low aspect ratio 580/70R38 tractor drive tyre on a loose sandy loam overlying a hardpan were measured by Way *et al.* (2000). The interface pressures were concentrated more at the middle of a lug and at the edge of the tread than near the centreline of the tyre when the tyre inflation pressure was 40 kPa and the corresponding correct load was used. When the inflation pressure was 120 kPa and the corresponding correct load was used, the interface pressures were distributed more uniformly among the three sensor locations used on one lug. When the dynamic load was increased from 17 to 31 kN and the inflation pressure was increased from 40 to 120 kPa, changing from one correctly inflated condition to another, the tyre footprint area increased by only 3%.

Soil–tyre interface pressures for an 18·4R38 tractor drive tyre on a loose sandy loam and a loose clay loam were presented as contour graphs by Raper *et al.* (1995a). They found that increases in inflation pressure at constant dynamic load decreased rut width, total contact length, and total contact area of the tyre, but caused the soil–tyre interface pressures to increase overall. Increases in dynamic load at constant inflation pressure increased rut width, rut cross-sectional area, and soil–tyre interface pressures.

Burt *et al.* (1989) reported that the normal stress distribution at the soil–tyre interface for a radial-ply R-1 tractor drive tyre on loose and firm soil overlying a hardpan was extremely non-uniform across the tyre width and along the soil–tyre contact arc. In general, the normal stress at the soil–tyre interface varied with changes in dynamic load. Other research has shown the effects of inflation pressure and dynamic load on

Notation

h	vertical distance from axle centre to horizontal section of path of a pressure sensor mounted on the tyre tread, mm	z	rut depth for a pressure sensor on the tyre tread, mm
r_u	radius from axle centreline to centre of pressure sensor diaphragm when tyre tread was undeflected, mm	θ_f	angle between a vertical line extending downward from the axle centreline and a line extending from the axle centreline to the point where a pressure sensor on the tyre tread first contacted the soil, deg
V	forward velocity of wheel, m s^{-1}		
x_f	longitudinal distance from the axle centreline to the point where a pressure sensor lost contact with the soil, mm	θ_r	angle between a vertical line extending downward from the axle centreline and a line extending from the axle centreline to the point where a pressure sensor on the tyre tread lost contact with the soil, deg
x_r	longitudinal distance from the axle centreline to the point where a pressure sensor first contacted the soil, mm	ω	angular velocity of wheel, rad s^{-1}

soil–tyre interface pressures for agricultural tractor drive tyres (Jun *et al.*, 1997; Raper *et al.*, 1995b; Burt *et al.*, 1992; Wood & Burt, 1987).

Little information describing soil–tyre interface pressures for agricultural tractor drive tyres on structured soil is available, but such information would be useful in improving the understanding of tractive and soil compaction characteristics of tyres. Therefore, a project with the following objectives was conducted:

(1) to determine soil–tyre interface pressures of a radial-ply tractor drive tyre on structured clay soil and compare them with pressures on a loose sandy loam and a loose clay loam;
(2) to determine estimates of tyre footprint areas occurring while a radial-ply tractor drive tyre operates at 10% travel reduction on a structured clay, a loose sandy loam, and a loose clay loam; and
(3) to determine relationships between soil–tyre interface pressures and the net traction and tractive efficiency for a radial-ply tractor drive tyre on a structured clay, a loose sandy loam, and a loose clay loam.

2. Materials and methods

The experiment was conducted at the National Soil Dynamics Laboratory (NSDL), a facility of the United States Department of Agriculture, Agricultural Research Service in Auburn, Alabama, USA using the NSDL single wheel traction research vehicle described by Burt *et al.* (1980). The traction research vehicle operates on the soil bins at the NSDL and was used to power an 18·4R38 Armstrong Hi-Traction Lug Radial (1-Star) R-1 tyre with new, unworn lugs. The tyre had 30 long lugs and 30 short lugs, and the mean lug height of the long lugs at the circumferential centreline of the tyre was 43 mm. The undeflected tyre had a section width of 480 mm, a section height of 395 mm, and an aspect ratio of 0·82.

Six pressure sensors were mounted on the tread, with three on the face of a long lug and three on the portion of the undertread on the trailing side of the long lug (*Fig. 1*). The Sensotec Model F Subminiature Pressure Transducers had diaphragm diameters of 9·7 mm and were mounted in grooves in the lug face and undertread, with their diaphragms flush with the lug face or undertread (Sensotec, Inc., Columbus, Ohio). The nominal capacities of the pressure sensors were 690 kPa for the sensors on the lug face and 350 kPa for the sensors on the undertread.

The experiment was conducted on three soil bins at the NSDL. At the time the experiment was conducted, the Hiwassee clay (a clayey kaolinitic thermic *Typic Rhodudults*) soil bin had not been tilled for approximately 3 years and few plants tended to grow on this outdoor soil bin, so the soil had developed aggregates and a bulk structure, and was free of plant material. The two other soils were those in two indoor soil bins. One was the Norfolk sandy loam soil (a fine loamy siliceous thermic *Typic Paleudults*) and the other was the Decatur clay loam soil (a clayey kaolinitic thermic *Rhodic Paleudults*). These two soils were prepared by first rotary tilling the soil to a depth of about 600 mm. A hardpan was formed across the whole area of each bin by using a single mouldboard plough followed by a rigid wheel operating in the plough furrow. The loose soil above the hardpan was leveled with a scraper blade after the hardpan was formed. The top of the hardpan was 288 mm beneath the loose surface of the Norfolk sandy loam and 324 mm beneath the loose surface of the Decatur clay loam. The depth of the loose soil for each of these two soils was considerably greater than the tyre

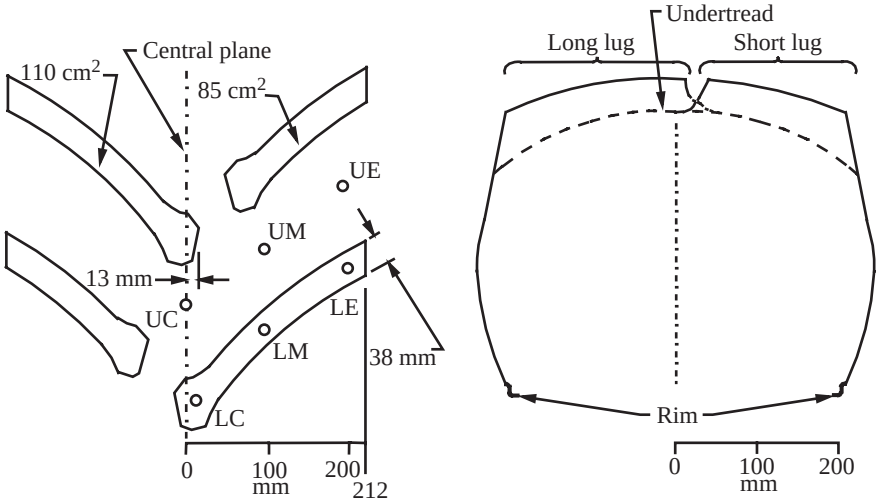

Fig. 1. Lug pattern of the tyre and locations of the six pressure sensors on the tread (left), and circumferential projections of lugs and undertread of unloaded tyre section onto a cross–sectional plane when inflation pressure was 110 kPa (right); LE, LM, and LC are lug interface pressures at the edge of the tread, at the middle of the lug, and near the centreline of the tyre, respectively; UE, UM, and UC are undertread interface pressures at the edge of the tread, at a position corresponding to the middle of a lug, and near the centreline of the tyre, respectively

lug height, so these two soils were considered to be loose, in terms of their effects on soil–tyre interface pressures. The particle size distributions were 23% sand, 17% silt, and 60% clay for the Hiwassee clay, 72% sand, 17% silt, and 11% clay for the Norfolk sandy loam, and 27% sand, 43% silt, and 30% clay for the Decatur clay loam. Mean soil cone index values determined using a cone penetrometer with a base area of 323 mm^2 (ASAE, 2001b) for a depth range of 0–100 mm in the undisturbed soil were 0·559, 0·437, and 0·867 MPa for the Hiwassee clay, Norfolk sandy loam, and Decatur clay loam, respectively. Other initial conditions of the soils are given in Table 1.

For all tests, the tyre forward velocity was 0·15 m s^{-1} and travel reduction (ASAE, 2001a) was 10%. Zero conditions for travel reduction calculations consisted of zero net traction (ASAE, 2001a) with the tyre operating on concrete. The forward velocity, dynamic load, travel reduction, and inflation pressure were controlled by computer throughout each test.

Three dynamic loads and their corresponding correct inflation pressures for a maximum speed of 40 km h^{-1} were used on the structured Hiwassee clay (Table 2). When the tyre was used on the loose Norfolk sandy loam and the loose Decatur clay loam, one dynamic load and the corresponding correct inflation pressure for a maximum speed of 32 km h^{-1} were used (Table 2). When comparisons of the 25·0-110 treatment results from either of the two loose soils are made with results of the 25·3-124 treatment in the structured clay, it is important to realise that while the dynamic loads

Table 1
Initial soil conditions

Soil	*Depth, mm*	*Water content, % dry basis**	*Dry bulk density, kg m^{-3}*
Structured Hiwassee clay	0–15	11·4	—
	100–140	22·1	1380
	220–260	23·0	1270
Loose Norfolk sandy loam	0–60	6·9	—
	124–164	6·9	1160
	298–338	7·0	1750
Loose Decatur clay loam	0–60	13·6	—
	142–182	13·8	1190
	334–374	13·9	1600

* Water content at maximum Proctor density is 23·6, 11·2, and 18·4 % dry basis for the Hiwassee clay, the Norfolk sandy loam, and the Decatur clay loam, respectively (Grisso, 1985).

Table 2
Dynamic load and inflation pressure combinations

Treatment	*Dynamic load, kN*	*Inflation pressure, kPa*
13·2–41*	13·2	41
19·8–83*	19·8	83
25·3–124*	25·3	124
25·0–110†	25·0	110

* Used on the structured Hiwassee clay soil. Load and inflation pressure combination is correct for a maximum speed of 40 km h^{-1}.

† Used on the loose Norfolk sandy loam and loose Decatur clay loam soils. Load and inflation pressure combination is correct for a maximum speed of 32 km h^{-1}.

were nearly equal, the inflation pressure of the 25·0-110 treatment was 89% of the inflation pressure of the 25·3-124 treatment.

3. Results and discussion

All results refer to soil–tyre interface pressures measured dynamically, as the tyre operated at 10% travel reduction. An example of soil–tyre interface pressure data for the six individual sensors on the tyre on the structured Hiwassee clay for the 25·3-124 dynamic load and inflation pressure treatment is shown in *Fig. 2*. The wheel angle data were adjusted so the value of 0 on the horizontal axis represents the bottom centre position for each pressure sensor, which was the position at which the sensor was directly below the axle. For each pressure sensor, pressures at positive wheel angles occurred when the sensor was forward of its bottom centre position and pressures at negative wheel angles occurred when the sensor was rearward of its bottom centre position.

The soil–tyre interface pressure data were used to develop graphs showing distributions of the contact pressures along the soil–tyre contact patch, and the peak contact pressures as the sensors passed through the contact patch (*Figs 3–7*). For each combination of soil, dynamic load, and inflation pressure, the four data sets, one for each replication, were examined. For each sensor, the mean angular position at which the sensor first contacted the soil, for the four replications, was determined. Similar means were calculated for the angular positions at which the sensors lost contact with the soil. These mean angle limits are the farthest forward and farthest rearward lines for each sensor (*Figs 3–7*). Each angular position range was then divided into 5° intervals forward and rearward from the bottom centre position. The mean contact pressures of these 5° intervals were calculated for each sensor for the four replications of each treatment. The 5° intervals were used for averaging because the angular position values of the four replications were not necessarily the same. For each sensor within each data set, the peak contact pressure and the angular position of the sensor at the peak pressure were determined. The arrows in *Figs 3–7* represent the means of the peak contact pressures for the four replications. The magnitude of each arrow is the mean of the peak contact pressures for the four replications and the angular position of the arrow is the mean angular position of the peak contact pressures.

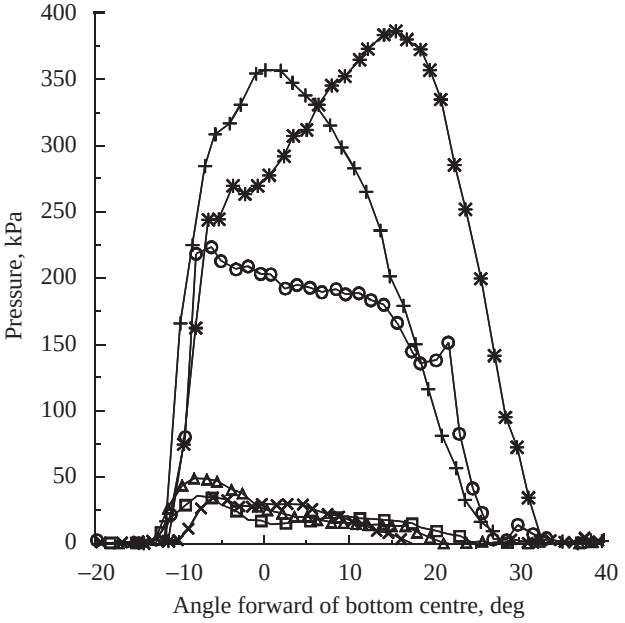

*Fig. 2. Soil–tyre interface pressures for one replication in the structured Hiwassee clay soil when the tyre dynamic load was 25·3 kN and the inflation pressure was 124 kPa: +, lug interface pressures at the edge of the tread; ○, lug interface pressures at the middle of the lug; *, lug interface pressures near the centreline of the tyre; ×, undertread interface pressures at the edge of the tread; Δ, undertread interface pressures near the middle of the lug; □ undertread interface pressures near the centreline of the tyre*

Soil structure in the structured Hiwassee clay caused the soil to resist penetration of the lugs, compared to a loose soil. Even the lowest load and inflation pressure treatment for the structured soil (13·2-41), however, caused the lugs to penetrate deeply enough to allow contact of a substantial portion of the undertread with the soil, as evidenced by the positive undertread pressures for several degrees of wheel angle (*Fig. 3b*).

For all five combinations of soil, dynamic load, and inflation pressure, the means and peaks of the interface pressures on the undertread were less than the tyre inflation pressure (*Figs 3–7*). The mean interface pressures for the 5° angle intervals show that for the structured Hiwassee clay, all three lug sensors for all three dynamic load and inflation pressure treatments had mean interface pressures that were considerably greater than inflation pressure for a substantial part of the contact patch. For the loose Norfolk sandy loam and the loose Decatur clay loam (*Figs 6* and *7*), the only lug sensor that had mean interface pressures greater than inflation pressure for a substantial part of the contact patch was the sensor near the lug edge of the tread (LE). The mean interface pressures on the undertread at the edge, middle of the lug and tyre centreline (UE, UM, and UC) for the 5° angle intervals in the loose Norfolk sandy loam are greater than those of any of the other four combinations of soil, dynamic load, and inflation pressure.

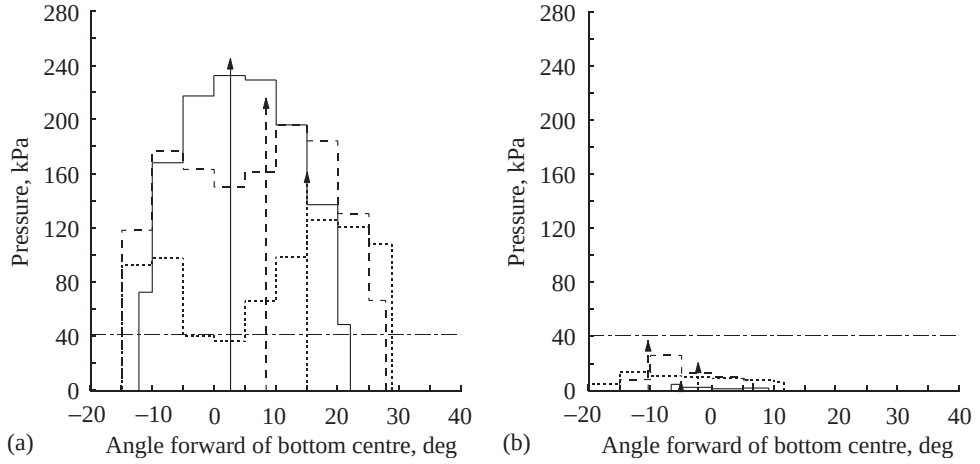

Fig. 3. Mean distributions of contact pressures for four replications on structured Hiwassee clay soil when the dynamic load was 13·2 kN and the tyre was correctly inflated to 41 kPa. Arrows indicate mean magnitudes and positions of the peak pressures for the four replications. The X–axis angles are the angular positions of the pressure sensors about the axle (zero angle indicates sensor was directly beneath axle): (a), lug face interface pressures; (b), undertread interface pressures; — – —, tyre inflation pressure. Left: —, lug interface pressures at the edge of the tread; — — —, lug interface pressures at the middle of the lug; – – –, lug interface pressures near the centreline of the tyre. Right: —, undertread interface pressures at the edge of the tread; — — —, undertread interface pressures at the middle of the lug;– – –, undertread interface pressures near the centreline of the tyre

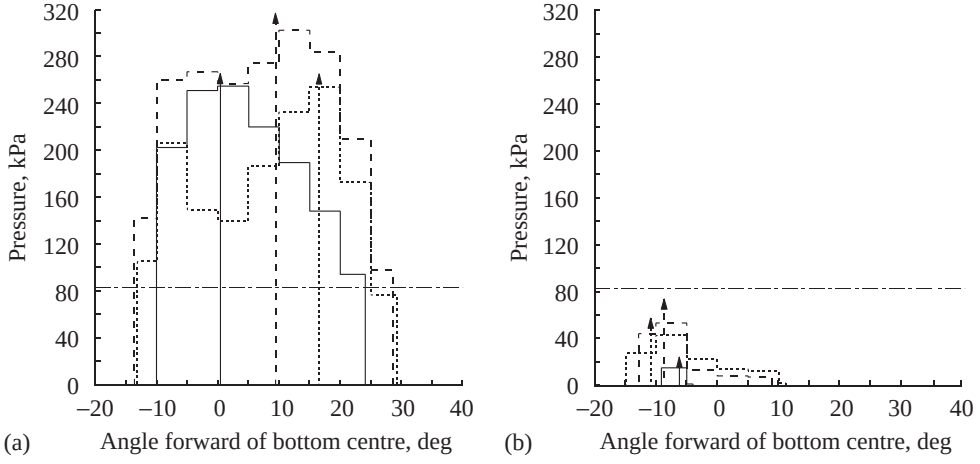

Fig. 4. Mean distributions of contact pressures for four replications on structured Hiwassee clay soil when the dynamic load was 19·8 kN and the tyre was correctly inflated to 83 kPa. Arrows indicate mean magnitudes and positions of the peak pressures for the four replications. The X-axis angles are the angular positions of the pressure sensors about the axle (zero angle indicates sensor was directly beneath axle): (a), lug face interface pressures; (b), undertread interface pressures; — – — , tyre inflation pressure. Left: —, lug interface pressures at the edge of the tread; — — —, lug interface pressures at the middle of the lug; – – –, lug interface pressures near the centreline of the tyre. Right: —, undertread interface pressures at the edge of the tread; — — —, undertread interface pressures at the middle of the lug;– – –, undertread interface pressures near the centreline of the tyre

Angular positions at which pressure sensors first contacted the soil and lost contact with the soil are useful in determining dimensions of the tyre footprint. For all three combinations of dynamic load and inflation pressure on the structured Hiwassee clay soil, the three pressure sensors on the tyre lug at the edge, middle of lug and tyre centreline (LE, LM, and LC) all first contacted the soil at angular positions from 22 to 30° forward of the bottom centre position (Table 3). The three sensors lost contact with the soil at angular positions from 10 to 15° rearward of the bottom centre position. For each of the sensors on the lug, as the combination of dynamic load and inflation pressure increased on the structured Hiwassee clay, the forward angular position limit increased. For each of the five combinations of soil, dynamic load, and inflation

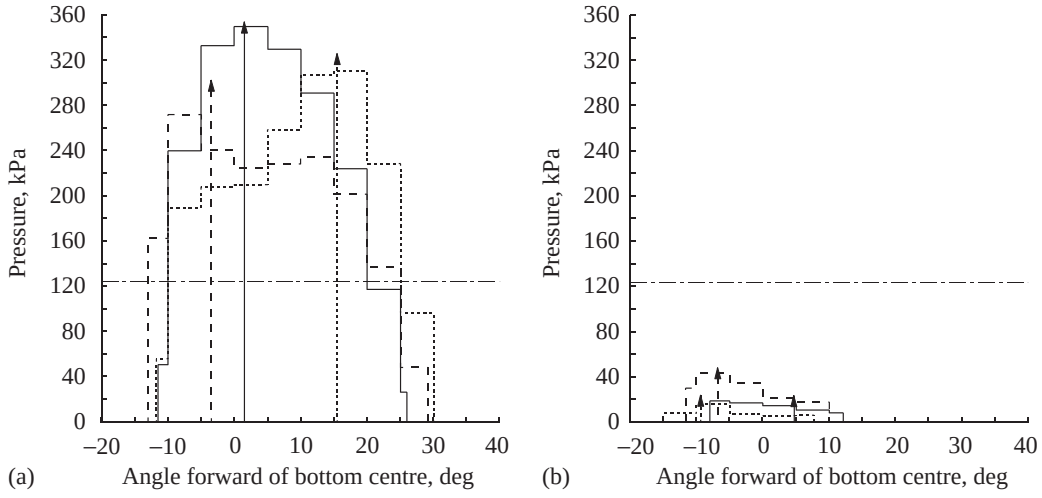

Fig. 5. Mean distributions of contact pressures for four replications on structured Hiwassee clay soil when the dynamic load was 25·3 kN and the tyre was correctly inflated to 124 kPa. Arrows indicate mean magnitudes and positions of the peak pressures for the four replications. The X-axis angles are the angular positions of the pressure sensors about the axle (zero angle indicates sensor was directly beneath axle): (a), lug face interface pressures; (b), undertread interface pressures; — – —, tyre inflation pressure. Left: —, lug interface pressures at the edge of the tread; — — —, lug interface pressures at the middle of the lug;– – –, lug interface pressures near the centreline of the tyre. Right: —, undertread interface pressures at the edge of the tread; — — —, undertread interface pressures at the middle of the lug;– – –, undertread interface pressures near the centreline of the tyre

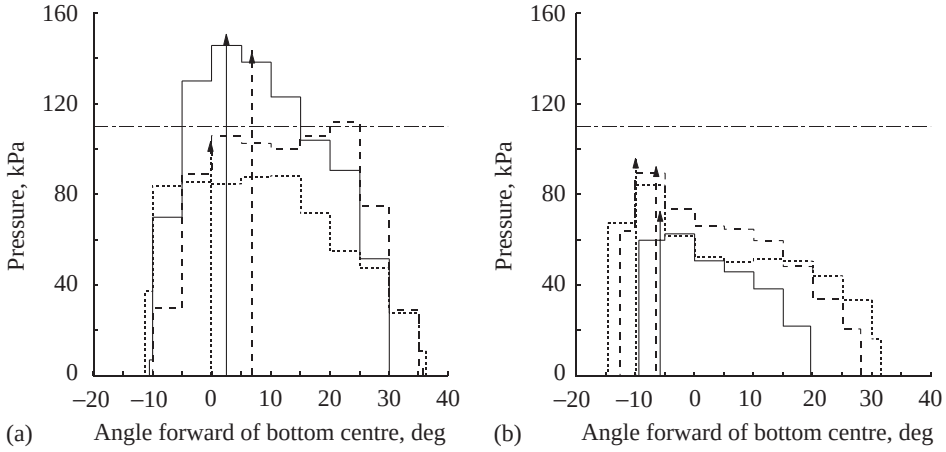

Fig. 6. Mean distributions of contact pressures for four replications on loose Norfolk sandy loam soil when the dynamic load was 25·0 kN and the tyre was correctly inflated to 110 kPa. Arrows indicate mean magnitudes and positions of the peak pressures for the four replications. The X-axis angles are the angular positions of the pressure sensors about the axle (zero angle indicates sensor was directly beneath axle): (a), lug face interface pressures; (b), undertread interface pressures; — – —, tyre inflation pressure. Left: —, lug interface pressures at the edge of the tread; — — —, lug interface pressures at the middle of the lug;– – –, lug interface pressures near the centreline of the tyre. Right: —, undertread interface pressures at the edge of the tread; — — —, undertread interface pressures at the middle of the lug;– – –, undertread interface pressures near the centreline of the tyre

pressure, the forward angular position limits for the sensors on the lug were greatest for the sensor near the tyre centreline (LC), were least for the sensor at the edge of the tread (LE), and were intermediate for the sensor near the middle of the lug (LM).

The peak interface pressure results show that the greatest ratio of peak interface pressure to inflation pressure was 5·98, occurring for the sensor on the lug near the edge of the tread (LE) for the 13·2-41 treatment on the structured Hiwassee clay soil (Table 4). The lowest ratio was 0.17 and occurred on the undertread sensor near the edge of the tread (UE) for the 13·2-41 treatment on the structured Hiwassee clay. On the structured Hiwassee clay soil, the peaks of the lug

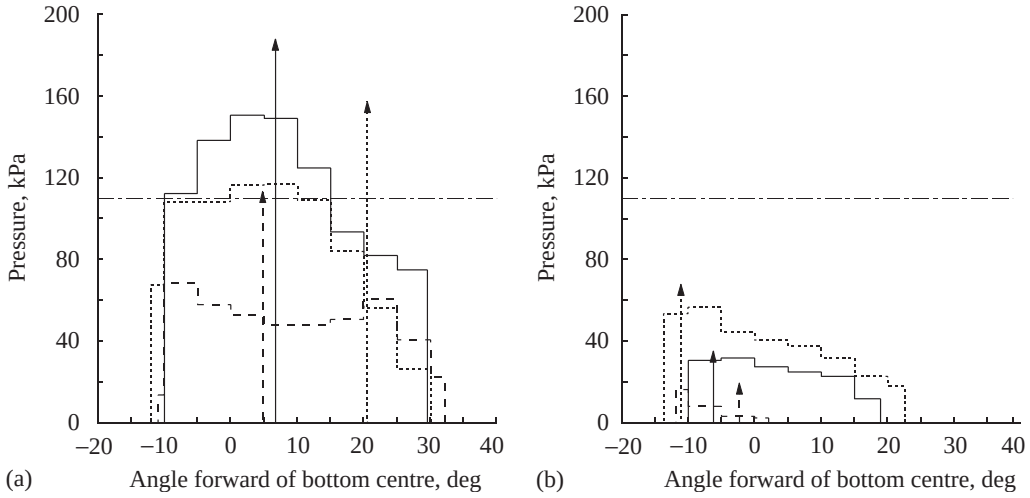

Fig. 7. Mean distributions of contact pressures for four replications on loose Decatur clay loam soil when the dynamic load was 25·0 kN and the tyre was correctly inflated to 110 kPa. Arrows indicate mean magnitudes and positions of the peak pressures for the four replications. The X-axis angles are the angular positions of the pressure sensors about the axle (zero angle indicates sensor was directly beneath axle): (a), lug face interface pressures; (b), undertread interface pressures; — – —, tyre inflation pressure. Left: —, lug interface pressures at the edge of the tread; — — —, lug interface pressures at the middle of the lug;– – –, lug interface pressures near the centreline of the tyre. Right: — undertread interface pressures at the edge of the tread; — — —, undertread interface pressures at the middle of the lug;– – –, undertread interface pressures near the centreline of the tyre

Table 3

Angular positions in degrees at which pressure sensors first contacted the soil ('Front') and lost contact with the soil ('Rear'), relative to the bottom centre position (0°)*; positive values are forward of, and negative values are to the rear of the bottom centre position

Pressure sensor†	*Angular positions of contact, degrees*									
	Structured Hiwassee clay						*Loose Norfolk sandy loam*		*Loose Decatur clay loam*	
	13·2–41		*19·8–83*		*25·3–124*		*25·0–110*		*25·0–110*	
	Front	*Rear*	*Front*	*Rear*	*Front*	*Rear*	*Front*	*Rear*	*Front*	*Rear*
LE	22·0	−12·2	24·1	−10·9	26·0	−11·5	30·3	−10·6	29·5	−9·9
LM	27·7	−14·9	28·6	−13·6	29·1	−13·0	35·7	−10·5	32·1	−10·9
LC	28·7	−14·9	29·3	−13·1	30·2	−11·7	36·3	−11·4	30·9	−12·0
UE	9·1	−6·7	−4·0	−9·1	12·1	−8·0	19·6	−9·4	18·9	−9·9
UM	6·5	−13·4	8·9	−12·8	10·4	−11·6	28·1	−12·6	2·1	−11·8
UC	11·5	−18·8	11·1	−14·8	7·7	−15·1	31·5	−14·6	22·5	−13·7

*The position for each pressure sensor when the sensor was directly beneath the axle centreline.

†LE, LM, and LC are the interface pressure sensors at the edge of the tread, at the middle of the lug, and near the centreline of the tyre, respectively; UE, UM, and UC are undertread interface pressures at the edge of the tread, at a position corresponding to the middle of a lug, and at the centreline of the tyre, respectively.

interface pressures exceeded inflation pressure and the mean pressures were greater than inflation pressure through most of the contact patch. On the loose Decatur clay loam, all peaks of the lug interface pressures exceeded inflation pressure. On the loose Norfolk sandy loam, the peaks for the lug sensors at the edge of the tread (LE) and at the middle of the lug (LM) exceeded the tyre inflation pressure, but the peak for the lug sensor near the tyre centreline (LC) was 94% of inflation pressure.

The peak interface pressures on the lug for the structured Hiwassee clay show that for the sensor at the edge of the tread (LE), the peak occurred near the bottom centre position, 0°. For the sensor on the lug near the centreline of the tyre (LC), the peak occurred when the sensor was approximately 15° forward of bottom centre. This LC sensor peak location probably was caused by the tendency for the carcass stiffness of the tyre to resist deflection as the tread contacted the soil. No particular patterns were found for the angular

Table 4
Peak soil–tyre interface pressures in kPa and ratios of peaks to the tyre inflation pressure

Pressure sensor[*]	*Structured Hiwassee clay*						*Loose Norfolk sandy loam*		*Loose Decatur clay loam*	
	13·2-41		*19·8-83*		*25·3-124*		*25·0-110*		*25·0-110*	
	Peak,[†] *kPa*	*Ratio*[‡]	*Peak, kPa*	*Ratio*	*Peak, kPa*	*Ratio*	*Peak, kPa*	*Ratio*	*Peak, kPa*	*Ratio*
LE	245	5·98	266	3·20	354	2·85	151	1·37	188	1·71
LM	216	5·27	317	3·82	302	2·44	144	1·31	113	1·03
LC	161	3·93	265	3·20	326	2·63	104	0·94	158	1·43
UE	7	0·17	24	0·29	23	0·19	73	0·66	35	0·32
UM	37	0·91	74	0·89	48	0·39	92	0·84	20	0·18
UC	21	0·51	58	0·69	24	0·19	96	0·87	68	0·62

[*] LE, LM, and LC are the interface pressure sensors at the edge of the tread, at the middle of the lug, and near the centreline of the tyre, respectively. UE, UM, and UC are undertread interface pressures at the edge of the tread, at a position corresponding to the middle of a lug, and at the centreline of the tyre, respectively.
[†] Mean of the peak interface pressures for the four replications.
[‡] Ratio of peak interface pressure to the inflation pressure.

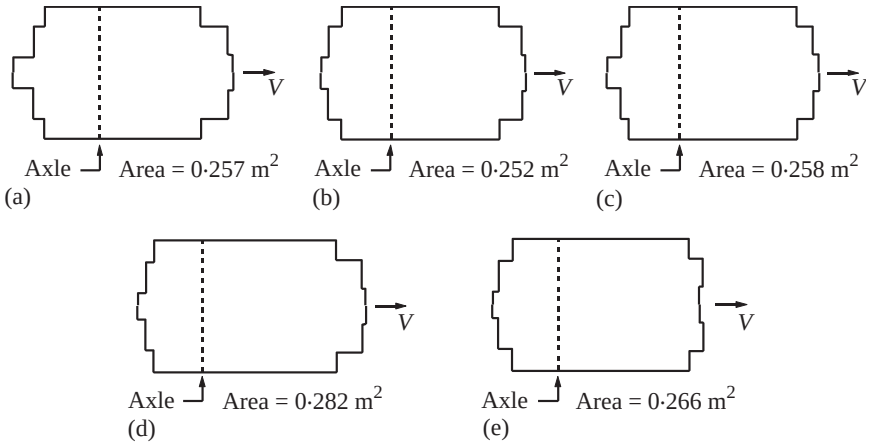

Fig. 8. Top views of the estimated footprints for the 18·4R38 radial-ply tyre for the following combinations of dynamic load, inflation pressure, and soil (a) the 13·2-41 treatment on the structured Hiwassee clay, (b) the 19·8-83 treatment on the structured Hiwassee clay, (c) the 25·3-124 treatment on the structured Hiwassee clay, (d) the 25·0-110 treatment on the loose Norfolk sandy loam, and (e) the 25·0-110 treatment on the loose Decatur clay loam. The velocity vector 'V' denotes the tyre direction of travel

positions of the sensors at which the peak interface pressures occurred for (a) all other sensors in the structured Hiwassee clay and (b) all six sensors in the loose Norfolk sandy loam and loose Decatur clay loam. The mean interface pressures for the 5° angle intervals on the structured Hiwassee clay generally increased as the dynamic load and inflation pressure increased.

The area of the projection of the tyre footprint onto a horizontal plane was estimated for each of the five combinations of dynamic load, inflation pressure, and soil. These are estimates of the footprint areas occurring while the tyre was operating at 10% travel reduction. The area estimates were calculated using the tyre dimensions, the penetration depth of the tyre tread into the soil, and the soil–tyre interface pressure data (see Appendix A). For each of the five combinations of soil, dynamic load, and inflation pressure, dimensions of an average tyre footprint were estimated. Five longitudinal strips comprised each footprint (*Fig. A1* in Appendix A). In four of the five estimated footprints [*Fig. 8*(*a*)–(*d*)], the longitudinal strip at the centreline of the footprint extended farther forward than the strip on either side of the centreline strip, and this was expected due to the convex curvature of the tread as shown in the cross-section in *Fig. 1*. The variability in the soil–tyre interface pressure data in the Decatur clay loam tended to be greater than that in the Hiwassee clay and Norfolk sandy loam soils due to the individual soil aggregates and the voids between those aggregates in the Decatur clay loam. This greater variability in the Decatur clay loam data probably caused the forward edge of the centreline strip to be rearward of the forward edges of

Table 5
Longitudinal distances from axle to front and rear edges of tyre footprint, mm

Extent of tyre footprint, mm									
Structured Hiwassee clay						*Loose Norfolk sandy loam*		*Loose Decatur clay loam*	
13·2-41		*19·8-83*		*25·3-124*		*25·0-110*		*25·0-110*	
Front	*Rear*	*Front*	*Rear*	*Front*	*Rear*	*Front*	*Rear*	*Front*	*Rear*
424	281	432	223	444	234	523	206	465	210

Table 6
Net traction and tractive efficiency means at 10% travel reduction

	Structured Hiwassee clay			*Loose Norfolk sandy loam*	*Loose Decatur clay loam*
	13·2-41	*19·8-83*	*25·3-124*	*25·0-110*	*25·0-110*
Net traction, kN	4·7	7·1	8·9	11·5	11·0
Tractive efficiency, %	77·3	76·1	75·1	76·6	73·5

the strips on each side of the centreline strip for the footprint in the loose Decatur clay loam [*Fig. 8*(*e*)].

The footprint area estimates for the three dynamic load and inflation pressure treatments in the structured Hiwassee clay were nearly equal (*Fig. 8*). This was unexpected because the rut depths at the tyre centreline increased as the dynamic load and inflation pressure increased (Table A1 in Appendix A). This finding, however, is similar to results on a loose sandy loam soil reported by Way *et al.* (2000) which showed the estimated footprint area increased by only 3% when the dynamic load was increased from 17 to 31 kN and the inflation pressure was increased from 40 to 120 kPa, changing from one correctly inflated condition to another. The footprint area estimates for the loose Norfolk sandy loam and loose Decatur clay loam (*Fig. 8*) were 10 and 4% greater, respectively, than the mean area of the three structured Hiwassee clay treatments, which was 0·256 m^2.

The forward and rearward extents of the tyre footprints, relative to the axle, are given in Table 5. The tyre footprint on the loose Norfolk sandy loam soil extended farther forward relative to the axle than the footprint for any of the three combinations of dynamic load and inflation pressure on the structured Hiwassee clay or the footprint on the loose Decatur clay loam soil. This greater forward extension of the footprint relative to the axle in the loose sandy loam, compared to the structured clay, probably resulted from the greater sinkage depth in the sandy loam.

The constant travel reduction value of 10% caused the net traction developed by the tyre to increase as the combination of dynamic load and inflation pressure increased for the three treatments on the structured Hiwassee clay (Table 6). Net traction values on the loose Norfolk sandy loam and loose Decatur clay loam were greater than the net traction for the 25·3-124 treatment on the structured Hiwassee clay. The greater uniformity in the soil–tyre interface pressures on the loose soils, relative to the uniformity on the structured Hiwassee clay, probably contributed to this difference. Tractive efficiency (ASAE, 2001a) was relatively constant for all five combinations of soil, dynamic load, and inflation pressure (Table 6), so differences in magnitudes and distributions of soil–tyre interface pressures caused no apparent differences in tractive efficiency.

4. Conclusions

The following conclusions were drawn.

(1) Soil–tyre interface pressures for a radial-ply tractor drive tyre operating at 10% travel reduction varied, depending on the soil condition, dynamic load, and inflation pressure. On a structured clay soil, interface pressures on a lug face were substantially greater than tyre inflation pressure and those on the undertread were considerably less than inflation pressure. On a loose sandy loam and a loose clay loam, some interface pressures on the lug face exceeded inflation pressure by only a small amount and others were a small amount less than inflation pressure, while undertread pressures were less than inflation pressure.

(2) Estimated tyre footprint areas occurring while the tyre ran at 10% travel reduction were nearly equal for three correctly inflated load and inflation pressure combinations on a structured clay soil. The estimated footprint area for the tyre with a dynamic load of 25 kN,

an inflation pressure of 110 kPa, and 10% travel reduction on a loose sandy loam was 10% greater, and on a loose clay loam was 4% greater, than the average of the three footprint areas on the structured clay soil.

(3) The net traction developed by the tyre on a loose sandy loam and a loose clay loam was greater than the net traction developed on a structured clay when the dynamic load and inflation pressure on the structured clay were similar to those on the loose soils. Greater uniformity in the soil–tyre interface pressures on the loose soils, relative to the uniformity on the structured clay, probably contributed to this difference. Differences in magnitudes and distributions of soil–tyre interface pressures for three combinations of dynamic load and inflation pressure on a structured clay soil and one combination on a loose sandy loam and a loose clay loam caused no apparent differences in tractive efficiency.

References

ASAE (2001a). S296·4 DEC01. General terminology for traction of agricultural tractors, self-propelled implements and traction and transport devices. ASAE Standards (48th Edn.)

ASAE (2001b). S313·3 FEB99. Soil cone penetrometer. ASAE Standards (48th Edn.)

Burt E C; Reaves C A; Bailey A C; Pickering W D (1980). A machine for testing tractor tires in soil bins. Transactions of the ASAE, **23**(3), 546–547, 552

Burt E C; Wood R K; Bailey A C (1989). Effects of dynamic load on normal soil–tire interface stresses. Transactions of the ASAE, **32**(6), 1843–1846

Burt E C; Wood R K; Bailey A C (1992). Some comparisons of average to peak soil–tire contact pressures. Transactions of the ASAE, **35**(2), 401–404

Grisso R D (1985). Compaction of agricultural soil by continuous deviatoric stress. PhD Dissertation, Auburn University, Auburn, Alabama, USA

Jun H; Taniguchi T; Kishimoto T; Yoshida M; Tamari T (1997). Measurement of tire–lug contact stresses by a three-dimensional stress transducer. Journal of Japanese Society of Agricultural Machinery, **59**(6), 3–10

Raper R L; Bailey A C; Burt E C; Way T R; Liberati P (1995a). Inflation pressure and dynamic load effects on soil deformation and soil–tire interface stresses. Transactions of the ASAE, **38**(3), 685–689

Raper R L; Bailey A C; Burt E C; Way T R; Liberati P (1995b). The effects of reduced inflation pressure on soil–tire interface stresses and soil strength. Journal of Terramechanics, **32**(1), 43–51

Way T R; Kishimoto T; Burt E C; Bailey A C (2000). Soil–tire interface pressures of a low aspect ratio tractor tire. In: Subsoil Compaction: Distribution, Processes and Consequences (Horn R; van den Akker J J H; Arvidsson J, eds), Advances in GeoEcology, Vol. 32, pp 82–92. Catena Verlag GMBH, Reiskirchen, Germany

Wood R K; Burt E C (1987). Soil–tire interface stress measurements. Transactions of the ASAE, **30**(5), 1254–1258

Appendix A Procedure for calculating estimated horizontal areas of tyre footprints

The projection of the tyre footprint onto a horizontal plane was approximated as five strips (*Fig. A1*). The dimensions of the strips, and therefore the area of the tyre footprint, were estimated using the tyre dimensions, the penetration depth of the tyre tread into the soil, and the soil–tyre interface pressure data. The following procedure was used.

(1) Each pressure sensor on the tyre tread was assumed to be in contact with the soil when its pressure data were positive. The pressure sensor data and wheel angular position data were used to determine the angular position of each sensor when the pressure sensor first contacted the soil at the forward edge of the tyre footprint and when the sensor lost contact with the soil at the rearward edge of the footprint. These angles were referenced relative to the bottom centre position, which was the position when the sensor was directly beneath the centreline of the axle. Four replications were done for each combination of dynamic load, inflation pressure, and soil, so the mean forward and mean rearward angular position limits were determined for each pressure sensor for the four replications of each combination of dynamic load, inflation pressure, and soil. For example, for the 25·3-124 dynamic load and inflation pressure combination on the structured Hiwassee clay soil, the forward angular position limit of the LC pressure sensor was 30·2° forward of the bottom centre position and the rearward limit was 11·7° rearward of the bottom centre position (Table 3).

(2) When viewed from the right-hand side of the tyre, the path of each pressure sensor relative to a reference frame moving forward with the axle was assumed to consist of a straight horizontal line for a certain fore-aft length beneath the axle and a circular arc whose centre was the axle centre, for the remainder of the path (*Fig. A2*). Measurements of the rut depth at imprints of lugs and the undertread, relative to the undisturbed soil surface, were made after the tyre was operated on the soil. For example, the depth of the imprint of the LC pressure sensor was assumed to be the depth of the lug imprint portion of the rut near the tyre centreline, which was 71 mm for the 25·3-124 dynamic load and inflation pressure combination on the structured Hiwassee clay soil (Table A1). The vertical distance from the undisturbed soil surface to the horizontal line that extends to the right from Point B in *Fig. A1* was assumed to be the rut depth that corresponded to the particular pressure sensor, so in this example, this distance z was 71 mm.

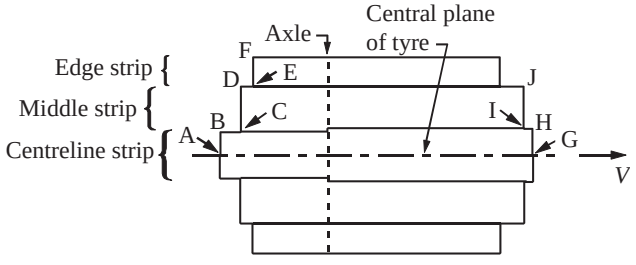

Fig. A1. Top view showing the five strips comprising the estimated footprint for the 18·4R38 radial-ply tyre at the 25·3-124 tyre load and inflation pressure combination on the structured Hiwassee clay soil. The footprint is symmetrical about the tyre central plane. The velocity vector 'V' denotes the tyre direction of travel

Table A1
Depth of rut at each soil–tyre interface pressure sensor mounted on the tyre lug, mm

Sensor[*]	*Rut depth, mm*				
	Structured Hiwassee clay			*Loose Norfolk sandy loam*	*Loose Decatur clay loam*
	13·2-41	*19·8-83*	*25·3-124*	*25·0-110*	*25·0-110*
LE	36	48	42	90	100
LM	37	53	57	100	110
LC	38	57	71	110	120

[*] LE, LM, and LC are lug interface pressure sensors at the edge of the tread, at the middle of the lug, and near the centreline of the tyre, respectively.

Table A2
Locations of soil–tyre interface pressure sensors on the undeflected tread of the 18·4R38 tyre

Sensor[*]	*Radius, mm*[†]	*Lateral distance, mm*[‡]
LE	853	197
LM	875·5	99
LC	883·5	13
UE	816	166
UM	838	83
UC	844	0

[*] LE, LM, and LC are lug interface pressure sensors at the edge of the tread, at the middle of the lug, and near the centreline of the tyre, respectively; UE, UM, and UC are pressure sensors on the undertread at lateral positions that correspond to those of LE, LM, and LC, respectively.
[†] Radius from centreline of axle to centre of pressure sensor.
[‡] Lateral distance from central plane of tyre to centre of pressure sensor.

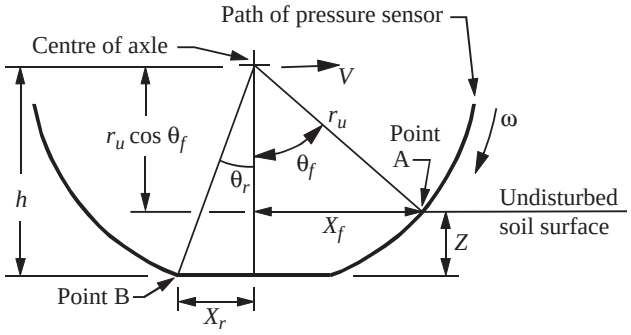

Fig. A2. Side view of the path of a pressure sensor mounted on the tyre tread, as viewed from a reference frame moving forward with the axle. Bold line represents the path for one pressure sensor. The sensor was assumed to first contact the soil at point A and to depart from the soil at point B; h, height of axle centre above horizontal section of tread pressure sensor path; z, rut depth for tread pressure sensor; r_u, undeflected tyre radius at pressure sensor; x_f and x_r, longitudinal distances from axle centreline to front and rear edges of contact patch; θ_f and θ_r, angles from vertical line extending downward from axle to the forward and rearward edges of the contact patch; ω, angular velocity of wheel; V, forward velocity of wheel

The longitudinal distance from the axle centreline to the point where the pressure sensor first contacted the soil x_f and that from the axle centreline to the point where the pressure sensor lost contact with the soil x_r were calculated as

$$x_f = r_u \sin \theta_f \quad \text{(A1)}$$

where: r_u is the radius in mm from axle centreline to centre of pressure sensor diaphragm when tyre tread was undeflected; θ_f is the forward angular position limit in degrees; and

$$x_r = (r_u \cos \theta_f + z) \tan \theta_r \quad \text{(A2)}$$

where: z is the depth in mm of horizontal portion of pressure sensor path relative to undisturbed soil surface; and θ_r is the rearward angular position limit in degrees.

For each of the three pressure sensor location categories (edge, middle, and centreline), for each combination of dynamic load, inflation pressure, and soil, the longitudinal distance of the forward edge of the footprint strip forward of the axle was calculated based on the pressure data for both the lug sensor and the undertread sensor. Considering the strip representative of the sensors at the tyre centreline for this example, the radius from the axle centreline to the centre of the LC pressure sensor when the tyre tread was undeflected was 883·5 mm (Table A2). Using the LC pressure sensor forward angle limit in Eqn (A1), the longitudinal distance of the forward edge of the centreline footprint strip, relative to the axle centreline was $x_f = 883{\cdot}5 \sin(30{\cdot}2) = 444$ mm. The value of θ_f for the UC sensor was only 7·7° so the 444 mm value is the forward limit of this centreline strip in this example. The longitudinal distance of the rearward edge of this centreline strip in this example was calculated using Eqn (A2) for both the LC and UC pressure sensor rearward angle limits. The depth of the imprint of the LC pressure sensor relative to the undisturbed soil surface for the 25·3-124 combination of dynamic load and inflation pressure in the structured Hiwassee clay soil used in the following calculations was 71 mm (Table A1). For the LC limit, the distance was $x_r = [883{\cdot}5 \cos(30{\cdot}2) + 71] \tan(11{\cdot}7) = 173$ mm. The calculation for the UC limit includes the difference between the radius for the LC sensor and for the UC sensor, to account for the lesser rut depth at the UC sensor relative to the LC sensor. For this example, the radii for the LC and UC sensors were 883·5 and 844 mm, respectively (Table A2). So, for the UC limit, the distance was

$$x_r = [844 \cos(7{\cdot}7) + 71 - (883{\cdot}5 - 844)] \tan(15{\cdot}1) = 234 \text{ mm}$$

Comparing the LC value of 173 mm with the UC value of 234 mm, the UC value is greater, so it was used as the value

representing the longitudinal distance of the rearward edge of this centreline strip.

For all five combinations of dynamic load, inflation pressure, and soil, the forward limits of the footprint strips were governed by the LC, LM, and LE sensor forward limits. The rearward limit for the centreline and edge strips were governed by the UC and LE sensor rearward limits, respectively. The rearward limits for the middle strips for the three combinations of dynamic load and inflation pressure in the Hiwassee clay soil, were governed by the LM sensor rearward limits, and for the Norfolk sandy loam and Decatur clay loam soils, were governed by the UM sensor rearward limits.

(3) The layout of the footprint for the 25·3-124 dynamic load and inflation pressure combination on the structured Hiwassee clay soil is shown in *Fig. A1*. For each of the five combinations of dynamic load, inflation pressure, and soil, half of the width of the footprint, which was the distance from the central plane of the tyre to point F in *Fig. A1*, was assumed to be 212 mm. This was the lateral distance from the central plane of the tyre to the shoulder of a lug when the tread was undeflected. Point H is on the forward portion of the footprint, where the lug sensors governed the footprint dimensions, so point H was taken as the midpoint between LC and LM pressure sensors. Therefore, the lateral distance from the tyre central plane to point H was $(13+99)/2$ (Table A2), or 56 mm. Similarly, point J was taken as the midpoint between the LM and LE sensors, so the lateral distance from the tyre central plane to point J was $(99+197)/2 = 148$ mm. The lateral distance from the tyre central plane to point F was 212 mm. Dimensions of the footprint portion forward of the axle were governed by the lug sensors, whereas dimensions of the footprint portion to the rear of the axle were governed by a combination of the lug and undertread sensors. Rearward of the axle, the centreline strip was governed by the UC sensor and the middle strip was governed by the LM sensor, so point B was taken as the midpoint between the UC and LM sensors. Therefore, the lateral distance from the tyre central plane to point B was $(0+99)/2 = 49{\cdot}5$ mm. The edge strip rearward of the axle was governed by the LE sensor, so point D was taken as the midpoint between the LM and LE sensors. Therefore, the lateral distance from the tyre central plane to point D was $(99+197)/2 = 148$ mm.

The procedure used here generally overestimates the distance of the forward edge of each footprint strip forward of the axle and the distance of each strip rearward of the axle because the forward-most and rearward-most extents of the strips are used. For example, in step 2 above, the 234 mm value was used rather than the 173 mm value because the 234 mm value was greater. The procedure, however, underestimates the overall width of the estimated footprint because the lateral distance from the tyre central plane to the side of the footprint is estimated as the lateral distance from the central plane to the shoulder of the lug. Actually, as the tyre sinks into the soil, the fact that the outer surface of the lug at the soil surface is laterally outboard of the shoulder of the lug, means the lateral distance from the central plane to this line where the lug outer surface meets the soil surface is greater than the central plane-to-shoulder distance. This overestimating of the footprint strip lengths is thought to be offset by this underestimating of the overall width of the footprint, so the footprint area estimates are thought to be reasonably accurate.

Two additional sources of error are possible in the footprint area calculations. First, the assumption that the shape of each pressure sensor path (*Fig. A2*) is comprised of a circular arc and a horizontal line is not necessarily valid. The path is more likely to be a continuous curve. The assumed path shape, however, is believed to cause only a relatively small error in the footprint area calculations. Second, the assumption that no berm of soil develops at the forward edge of the footprint generally would not be valid in loose soil, but probably is more valid in structured soil. The existence or lack of such a berm, however, probably would affect the footprint area calculations only slightly.